The Cavitating Pump Rotordynamic Test Facility at ALTA S.p.A.: Upgraded Capabilities of a Unique Test Rig

G. Pace (g.pace@alta-space.com)
A. Pasini (a.pasini@alta-space.com)
L. Torre (l.torre@alta-space.com)
D. Valentini (d.valentini@alta-space.com)
L. d'Agostino (luca.dagostino@ing.unipi.it)

ALTA S.p.A, 56121 Ospedaletto, Pisa, Italy

ABSTRACT

The paper illustrates the upgrades recently introduced in Alta's Cavitating Pump Rotordynamic Test Facility in order to extend its experimental capabilities, with special reference to the addition of an auxiliary pump for testing of turbopump inducers over a wider range of flow coefficients, and the set-up of an original apparatus specifically designed for the characterization of the dynamic transfer matrices of cavitating inducers and turbopumps. Examples are presented of the improved capabilities of the facility.

NOMENCLATURE

Latin symbols

e	Whirl eccentricity [m]
f_R	Normalized rotordynamic radial force [-]
M	Main motor torque [N*m]
P	Main motor power [W]
p_1	Static pressure at pump inlet [Pa]
p_v	Vapor pressure of the liquid [Pa]
p_{t1}	Total pressure at pump inlet [Pa]
p_{t2}	Total pressure at pump outlet [Pa]
Δp	Static pressure rise [Pa]
$\dot{Q}$	Volumetric flow rate [m^3/s]
r_{T1}	Tip radius at pump inlet [m]
r_{T2}	Tip radius at pump outlet [m]
T	Flow temperature [°C]

Greek symbols

γ_{xy}	Coherence function [-]
ϕ	Flow coefficient [-]
σ	Cavitation number [-]
ρ	Fluid density [kg/m^3]
ψ	Head coefficient [-]
Ω	Pump rotational speed [rad/s]
ω	Whirl rotational speed [rad/s]

Acronyms

ASI Agenzia Spaziale Italiana (Italian Space Agency)
CPRTF Cavitating Pump Rotordynamic Test Facility
ESA European Space Agency

INTRODUCTION

Propellant feed turbopumps represent one of the most crucial components of all primary propulsion concepts powered by liquid propellant rocket engines because of the severe limitations associated with the design of high power density, dynamically stable machines capable of meeting the extremely demanding suction, pumping and reliability requirements of space transportation systems. Cavitation is the major source of degradation of the suction performance, reliability, power density and useful life of this kind of turbopumps, and the cause of other equally undesirable effects such as the reduction of the overall efficiency and the drastic increase of the noise level ([1]). Cavitation can also provide the necessary flow excitation, compliance and load-dependence for triggering dangerous rotordynamic and/or fluid mechanic instabilities of the turbopump ([2], [3], [4], [5], [6], [7] and [8]), or even, through the coupling with thrust generation, of the entire propulsion system (POGO auto-oscillations of liquid propellant rockets, [15]). The occurrence of flow instabilities like rotating cavitation has been extensively reported in the development of

most of the high performance liquid propellant rocket fuel feed systems, including the Space Shuttle Main Engine ([17]), the European Ariane 5 engine ([18]) and the LE-7 engine of the H-II and H-II-A Japanese rockets ([19]). A few years ago, Japanese researchers postulated that the resonance of higher-order surge instabilities with the first bending mode of the inducer blades was responsible for the fatigue failure of the liquid hydrogen pump inducer of the 8th launch of H-II rocket in November 1999 ([20]). The combined effects of rotordynamic fluid forces and cavitation represent the dominant fluid mechanical phenomena that adversely affect the dynamic stability and pumping performance of high power density turbopumps ([9]). The most critical rotordynamic instability in turbopumps is the development of self-sustained lateral motions (*whirl*) of the impeller under the action of destabilizing forces of mechanical or fluid dynamic origin. Because of their greater complexity, rotordynamic fluid forces have so far received relatively little attention in the open literature, despite of their well recognized potential for promoting rotordynamic instabilities of high performance turbopumps ([10]) and for significantly modifying, in conjunction with cavitation, the dynamic properties of the impeller, and therefore the critical speeds of the whole machine ([5], [6], [7], [8], [11], [12], [13] and [14]).

Nowadays, experimentation still plays an essential role for technology progress of high performance turbopumps, because the extreme complexity and imperfect understanding of the relevant unsteady fluid dynamic phenomena prevent the possibility of relying on theoretical or numerical predictions alone. Operational and economic limitations clearly indicate that detailed experiments can only be effectively carried out on scaled turbopump models under fluid dynamic and thermal cavitation similarity. In recognition of these aspects, ASI funded the realization of the Cavitating Pump Rotordynamic Test Facility (CPRTF), the first openly documented facility in Europe – and one of the few in the world – capable of carrying out the direct measurement of the unsteady rotordynamic fluid forces on scaled cavitating or noncavitating turbopumps ([16]).

EXPERIMENTAL APPARATUS

The CPRTF is a low-cost, versatile and instrumentable test facility, operating in water at temperatures up to 90 °C ([16]). It has been designed for general experimentation on noncavitating/cavitating turbopumps and test bodies in water under fluid dynamic and thermal cavitation similarity (Figure 1 and Figure 2). Water is the selected working fluid because of its easily handling and cheapness. Moreover its thermodynamic properties allow for scaling cavitating performance of cryogenic fluids (as liquid oxygen and liquid hydrogen) by taking into account the cavitation thermal effects. This can be obtained by regulating the water temperature in order to simulate a particular cryogenic propellant.

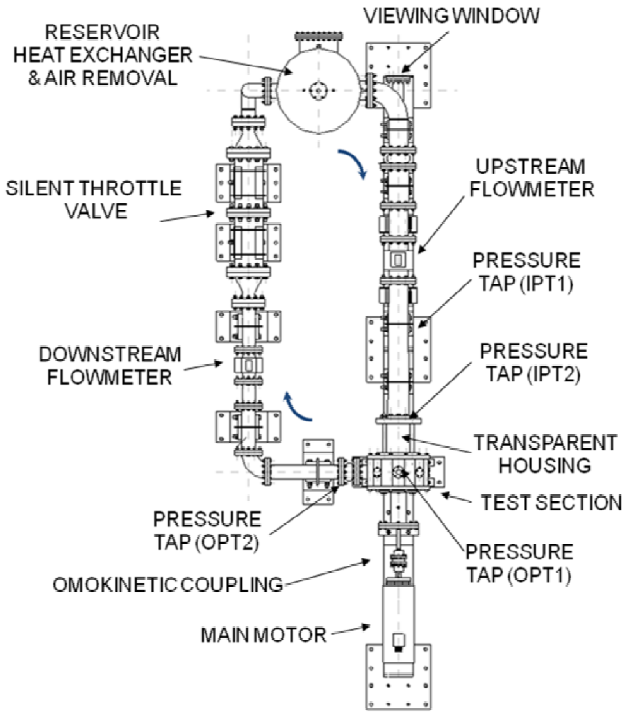

Figure 1 The CPRTF lay-out in ALTA S.p.A.

Figure 2 The Cavitating Pump Rotordynamic Test Facility in ALTA S.p.A. in the configuration used for tests on turbopumps ([22]).

The facility has been intended as a flexible apparatus that can readily be adapted to conduct experimental investigations on virtually any kind of fluid dynamic phenomena relevant to high performance turbopumps in a wide variety of alternative configurations (axial, radial or mixed flow, with or without an inducer). The CPRTF has been especially designed for the analysis of unsteady flow phenomena and rotordynamic forces in scaled cavitation tests under fluid dynamic and thermal cavitation similarity conditions. It can also be configured as a small water tunnel (Figure 3) to be used for thermal cavitation tests for experimental validation of numerical tools and simulations.

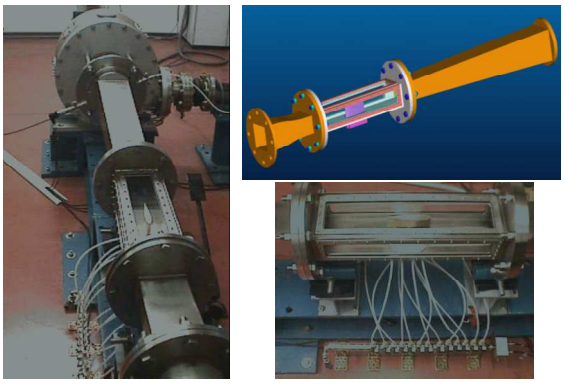

Figure 3 The Cavitating Pump Rotordynamic Test Facility in ALTA S.p.A. in the water tunnel configuration used for tests on hydrofoils ([21]).

For the tests on turbopumps the test section is like in Figure 4.

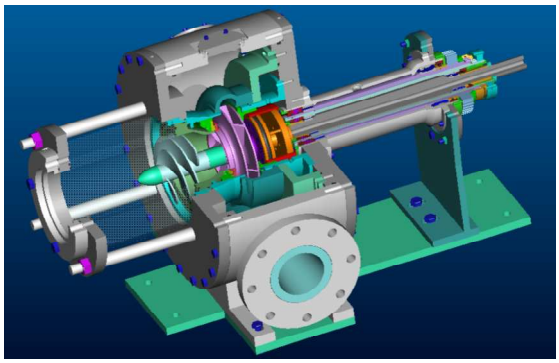

Figure 4 Cut-off of the CPRTF Test Section.

The system can be assembled in different configurations: inducer only, centrifugal pump only, or inducer and centrifugal pump together. The system, in all of its possible configurations, can be equipped with a rotating dynamometer (Figure 5) for the measurement of the forces and moments acting on the impeller.

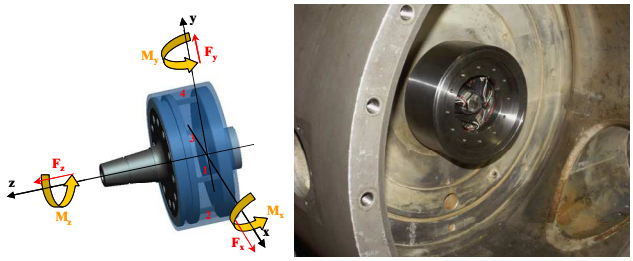

Figure 5 The rotating dynamometer. A schematic of the dynamometer is on the left, on the right the dynamometer mounted in the test chamber.

The rotating dynamometer is realized in one single piece of phase hardening steel AISI 630 H1025 and consists of two flanges connected by four square cross-section posts acting as flexible elements. The deformation of the posts is measured by 40 semiconductor strain gauges arranged in 10 full Wheatstone bridges, which provide redundant measurements of the forces and moments acting on the impeller. Each bridge is temperature self-compensated, with separate bipolar excitation and read-out for better reduction of cross-talking. The current design of the dynamometer is optimized for a suspended mass of 4 kg with 70 mm gyration radius, an added mass of about 2 kg (based on the expected magnitude of the rotordynamic forces), a rotational speed of 3000 rpm without eccentricity, and maximum rotational and whirl speeds up to 2000 rpm with 2 mm shaft eccentricity and 3:1 margin with respect to the first critical speed of the impeller mounted on the dynamometer. The driving shaft axis can be set in an eccentric position with respect to the nominal position by using a two-shafts mechanism (Figure 6).

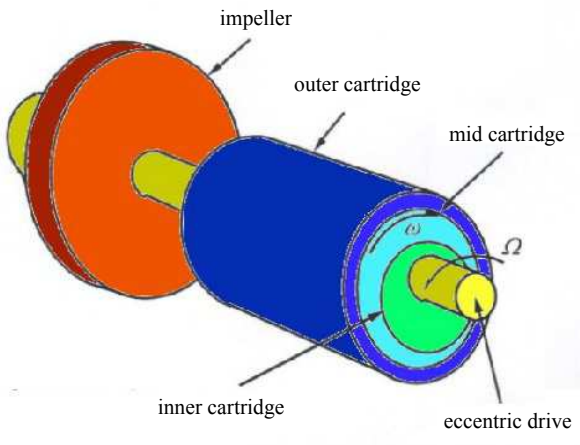

Figure 6 Schematic of the mechanism for adjusting the eccentricity of the driving shaft.

The shafts are mounted one inside the other and the eccentricity can be regulated in the range

between 0 and 2 mm by means of two eccentric holes, whose relative angular position can be finely adjusted from 0 to 2 mm before each rotordynamic test. The whirl motion is generated by a brushless motor driving the external shaft, while the impeller rotation is imparted by connecting the internal shaft to the main motor with an omokinetic coupling. The instantaneous absolute angular position (needed for rotordynamic tests) of both the shafts is controlled by two contrast sensors (Figure 7).

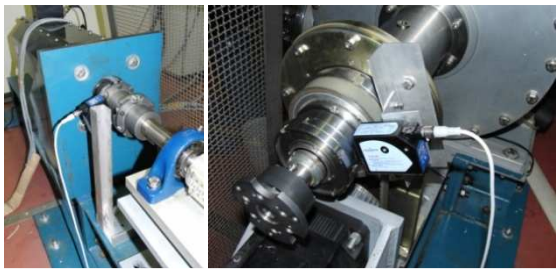

Figure 7 Contrast sensors for the measure of the absolute angular position of the driving shaft (left) and of the eccentric shaft (right).

The inlet plexiglas section is transparent in order to allow for the optical visualization of cavitation in the inducer. It can be instrumented with several flush-mounted piezoelectric pressure transducers (PCB M112A22, ICP® voltage mode-type, 0.1% class), located at three axial stations: inducer inlet, outlet and in correspondence of the blade tip (Figure 8), or possibly along the blade channels.

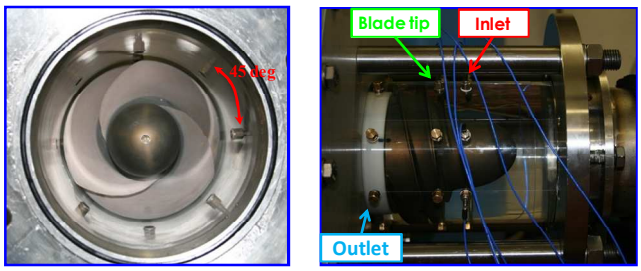

Figure 8 Axial position (on the right) and angular displacement (on the left) of the piezoelectric pressure transducers.

At each axial station up to eight transducers have been mounted with an angular spacing of 45 deg, in order to cross-correlate their signals for coherence and phase analysis, allowing for the detection, discrimination and analysis of up to four-lobed azimuthal flow instabilities. Waterfall plots of the power spectral density of the pressure fluctuations can be obtained as functions of σ, in order to identify the presence of flow instabilities in the flow. Cross-correlation of two pressure signals from different locations allows to determine the axial or azimuthal nature of each instability and, in the second case, the number of rotating cells involved.

The water pressure at the inlet of the test section can be adjusted by means of an air bag, while the temperature is regulated by a heat exchanger and an electrical resistance, all positioned in the tank. A Silent Throttle Valve, positioned in the discharge line, is used for the variation of the flow rate. Two electromagnetic flowmeters, mounted on the suction and discharge lines, provide the instantaneous measurement of the inlet and outlet flow rates. The inlet pressure is monitored by two absolute transducers mounted upstream of the test section, at different distances in order to take into account of the possible influence of the pre-rotation at low flow rates. Two pressure differential transducers are used for measuring the pump pressure rise. The characteristics of the CPRTF transducers are summarized in Table 1, where the location names refer to Figure 1.

Transducer	*Model*	*Range*	*Accuracy*	*Location*
absolute pressure transducers	PMP 1400 by Druck	0−1.5 bara	±0.25% FSO	IPT1/IPT2
differential pressure transducer	BMD 1P 1500 100 by Kulite	0−6.8 bard	± 0.1% FSO	+ tap: IPT1/IPT2 - tap: OPT1
flowmeter	by Fisher-Rosemount	0−100 l/s	± 0.5% FSO	suction and discharge lines
piezoelectric pressure transducers	M112A22 by PCB	0.007−345 kPa	± 0.1% FSO	on the inlet Plexiglas casing
resistance thermometer	PT100	0−100 ° C	±0.5° C	into the main tank
thermocouple	k-type	-40−375 ° C	±1.5° C	IPT1

Table 1 CPRTF sensors list.

Photo cameras and high-speed video cameras are used to allow for the optical visualization of the cavitating flow on the test item. In particular, side movies provide indications on the extension of cavitation in the blade channels, whereas frontal videos (Figure 9) give information on the radial and circumferential extension of the cavities on the blades.

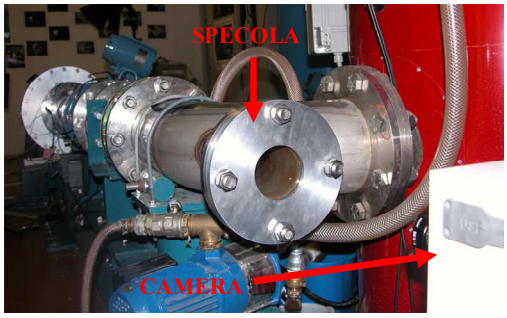

Figure 9 The optical access at the end of the facility suction line.

Table 2 summarizes the main operational parameters of the CPRTF.

Pump rotational speed	$\Omega = 0 \div 6000$ rpm
Main motor power	$P \le 30$ kW
Main motor torque	$M \le 100$ Nm
Suction pressure	$p_{t1} = 0.01 \div 6$ bar
Discharge pressure	$p_{t2} \le 11$ bar
Volumetric flow rate	$\dot{Q} \le 0.1$ m^3/s
Flow temperature	$T = 10 \div 90$ °C
Whirl eccentricity	$e = 0 \div 2$ mm
Whirl rotational speed	$\omega = -3000 \div 3000$ rpm
Impeller eye radius	$r_{T1} \le 90$ mm
Impeller outlet radius	$r_{T2} \le 112$ mm
Impeller outlet width	$b_2 \le 30$ mm

Table 2 Main specifications and operational parameters of the facility.

RECENT APPARATUS UPDATING

Recently the CPRTF capabilities have been upgraded in order to allow for the attainment of higher flow rates in inducer tests and to experimentally determine the dynamic transfer matrices of cavitating inducers and turbopumps by forcing the oscillation of the flow pressure at the pump inlet. In order to analyze the dynamic transfer matrices of cavitating pumps for the prediction and control of POGO oscillations in liquid propellant rockets, the set-up of the CPRTF has been modified. The CPRTF has been equipped with a vibrating table used for the generation of forced pressure oscillations by vertically oscillating the circuit reservoir at controllable frequency and amplitude of the oscillation. On the basis of earlier theoretical analyses ([28]), two geometrically independent configurations have been designed which indicated this choice as particularly appropriate for the experimental evaluation of the dynamic transfer matrices of cavitating inducers and turbopumps (Figure 10). Piezoelectric pressure transducers have been positioned along the circuit in order to measure pressure oscillations used for the evaluation of the dynamic transfer matrix of the pump. A picture of the CPRTF in its configuration with a longer discharge line is shown in Figure 11. The auxiliary pump (left) and the oscillating table supporting the pressure vessel (top-right) are also shown.

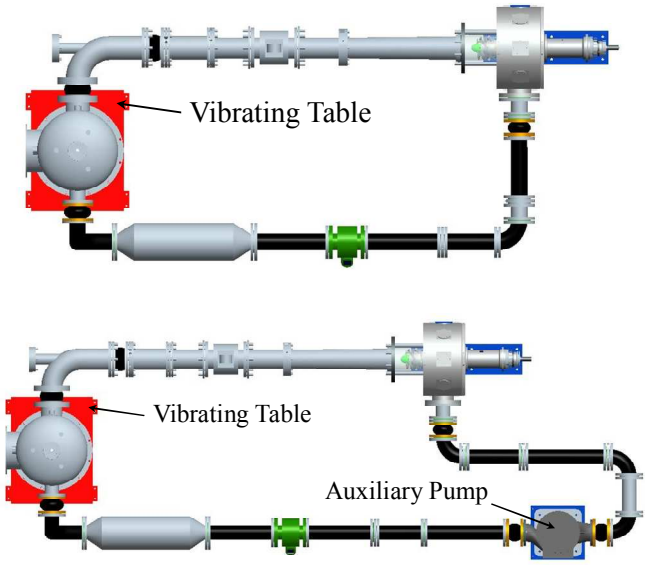

Figure 10 The two new set-up configurations ("short discharge line" configuration on top, "long discharge line" configuration on bottom) for the study of the dynamic transfer matrices of cavitating pumps. The vibrating table and the auxiliary pump are shown.

Figure 11 The CPRTF in its "long discharge line" configuration.

The characteristics of the oscillating table are shown in Table 3.

Direction of Vibration	Vertical
Maximum Vibration Frequency	50 Hz
Type of Electrical Motors	2-poles (2 motors)
Input Current	400 V, 3-phase
Motors Eccentricity	0.5 mm (0÷30 Hz) 0.25 mm (30÷50 Hz)
Amplitude of Vibrations	1 mm (0÷30 Hz) 0.5 mm (30÷50 Hz)
Maximum Load	500 kg
Supporting Plate Size	650 x 850 mm

Table 3 Main design characteristic of the oscillating table.

Higher flow rates can be reached with "long" configuration (Figure 10) by using the auxiliary pump (Grundfos TPE 100-390/2), whose main characteristics are summarized in Table 4.

Design Rotating Speed	2930 rpm
Design Flow Rate	178 m^3/hr
Design Head	32.9 m
Impeller Tip Diameter	169 mm
Connecting Flanges	DN100
Maximum Water Temperature	120 ° C
Maximum Water Pressure	16 bar
Motor Power (design)	22 kW
Motor Voltage	3 x 380÷480 V
Motor Current	43.5÷35 A
Pump Weight	247 kg

Table 4 Main design characteristics of Grundfos TPE 100-390/2.

EXPERIMENTAL CAPABILITIES

Several space rocket inducers have been tested and characterized in the CPRTF, with particular attention to their cavitating/noncavitating performance, the occurrence of flow instabilities and influence of thermal cavitation effects. In particular, two inducers used in the European Ariane 5 rocket turbopumps have been extensively studied in past activities ([23]): the four-bladed axial inducer MK1 inducer, a prototype of the liquid oxygen inducer of the Vulcain engine (first stage engine), and the two-bladed axial inducer FAST2, a prototype of the liquid oxygen inducer of the VINCI engine (second stage engine), both of them manufactured by Avio S.p.A. in Italy. In recent years an analytical model for designing high-head inducers has been developed at ALTA S.p.A. ([29], [30] and [31]) and some inducers realized on the basis of such a model (two three-bladed inducers, indicated as DAPAMITO3 and DAPAMITOR3 in Figure 12, and two four-bladed inducers indicated as DAPAMITO4 and DAPAMITOR4 in Figure 13) were successfully tested, confirming the performance predictions of the analytical model ([24]).

Figure 12 DAPAMITO3 (left) and DAPAMITOR3 (right).

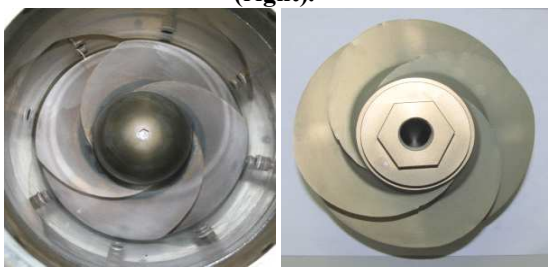

Figure 13 DAPAMITO4 (left) and DAPAMITOR4 (right).

The experimental capabilities of the CPRTF are summarized in the following.

Non-Cavitating Performance Characterization

The performance of inducers and impellers in non-cavitating conditions can be easily obtained, together with the possibility of varying the value of the clearance by substituting the plexiglas casing. A typical plot of the non-cavitating performance of inducers obtained in Alta's CPRTF is shown in Figure 14.

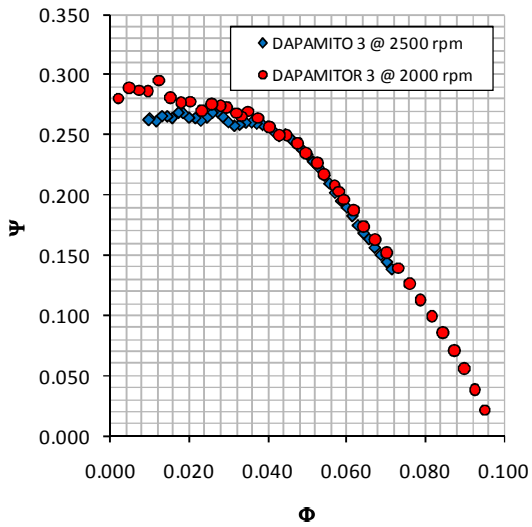

Figure 14 Non-cavitating pumping performance of inducers DAPAMITO3 and DAPAMITOR3 ([25]).

In the plot, $\Phi = Q/\pi\Omega r_T^3$ is the flow coefficient and $\Psi = \Delta p/\rho\Omega^2 r_T^2$ is static head coefficient. Tests on DAPAMITO3 have been carried out without the use of the auxiliary pump (not yet installed during the pertinent test campaign), whereas the tests on DAPAMITOR3 have been conducted with the help of the auxiliary pump. The results clearly illustrate the extended range of flow rates attainable by means of the auxiliary pump.

Cavitating Performance Characterization

The characterization of the cavitating performance of turbopumps have been carried out with two different procedures: either by stepping down the inlet pressure in a series of steady-state discontinuous tests, or by averaging the experimental results over relatively short shifting time windows while the inlet pressure is slowly ramped down in a continuous series of unsteady tests. In both of these cases the static head coefficient (Ψ) is plotted as function of the Euler number ($\sigma = \frac{p_1 - p_V}{\frac{1}{2}\rho\Omega^2 r_{T1}^2}$) in order to assess the head drop caused by cavitation development and determine the suction characteristics of the machine. In steady-state tests the static head coefficient is obtained for specific values of the inlet Euler number. Steady-state tests are so performed at constant inlet pressure, which is fixed by regulating the pressure inside the reservoir before the beginning of the test. In unsteady tests the pressure inside the reservoir is reduced during the test from a non-cavitating value to a minimum value limited by the water level in the tank above the axis of the pump. So it is possible to obtain in a single test all of the possible values of the static head coefficient. Figure 15 reports the results of the steady-state and continuous tests carried out on DAPAMITO3 inducer at ambient temperature and for an off-design value of the flow coefficient.

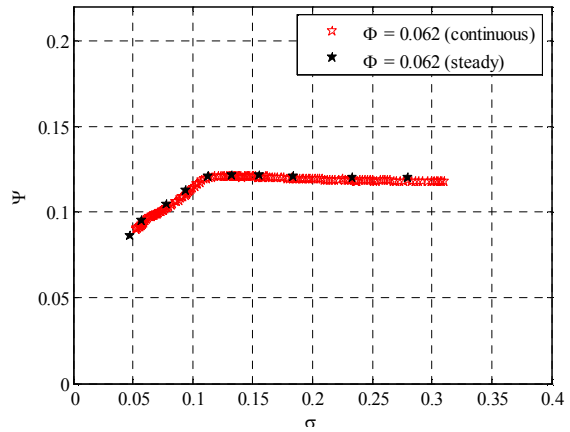

Figure 15. Results of the steady-state and continuous cavitation tests on the DAPAMITO3 inducer at ambient temperature.

Instability Analysis

Characterization of flow instabilities in terms of intensity, frequency and number of lobes is carried out by post-processing the pressure fluctuations measured by the PCB transducers mounted on the Plexiglas duct at the inlet of the cavitating inducer. The pressure signals are acquired and analyzed by means of Fast Fourier Transforms in order to obtain the spectrum of the oscillating phenomena occurring in the pump flow. All the spectra obtained at different Euler numbers are normally summarized in 3D plots (waterfall plots), where the amplitude of the spectrum is plotted against frequency and Euler number. The waterfall plots are normally filtered to eliminate the intense lines corresponding to the pump rotational frequency and its harmonics in order to highlight non-synchronous phenomena (Figure 16).

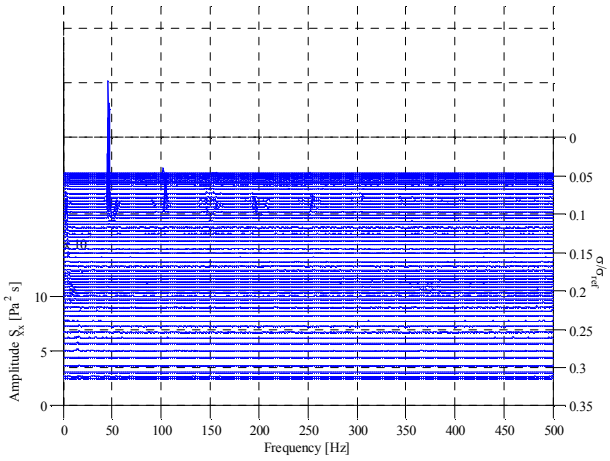

Figure 16 Waterfall plot of the spectrum of the inlet pressure fluctuations on DAPAMITO3 inducer at off design condition, filtered for the *n*Ω frequencies.

The spectrum is used to determine the frequency of all of the apparent flow phenomena, whereas

their nature is defined on the basis of the cross-spectrum phases for different couples of transducers. Axial phenomena are characterized by constant zero phase of the cross-spectrum; rotating phenomena generate cross-spectrum phases proportional to the angular spacing $\Delta\theta$ between the relevant transducers located at the same axial position and to the number of lobes n of the phenomenon. The statistical validation of the analysis is based on the value of the coherence function γ_{xy} between signals obtained from different transducers (only phenomena with values of γ_{xy} consistently larger than 0.8 are normally considered). An example of this analysis of flow instabilities is shown in Figure 17 where, for a fixed value of σ, the spectrum (top), the cross-spectrum (mid) and the coherence function (bottom) of the pressure signals from two transducers with 45° angular separation are plotted.

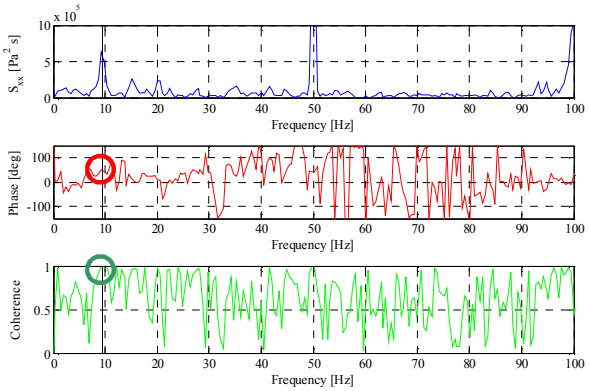

Figure 17 Amplitude of the spectrum, phase of the cross-spectrum and coherence function of the pressure signals of two transducers with 45° angular separation mounted at the inlet section of the DAPAMITO3 inducer, at off-design conditions.

The frequency of interest of the analysis is indicated by the vertical black line in the plots. The same analysis is repeated for different couples of transducers and is summarized in Figure 18, where the one-lobe nature of the phenomenon under investigation is evident.

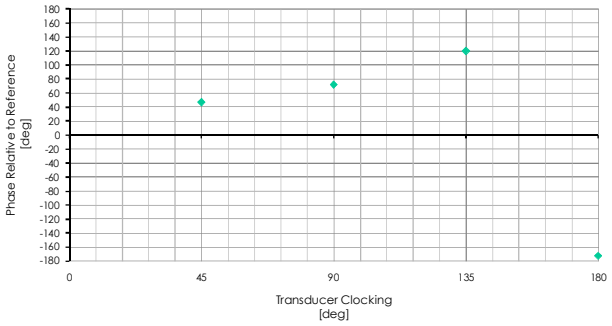

Figure 18 Cross-correlation phase as a function of the angular spacing between two considered transducers (transducer clocking) for the same conditions of Figure 17.

Visual Characterization of Cavitating Flows

One of the most interesting and advantageous aspects of cavitation consists in the possibility of visually characterizing its behavior by relatively simple optical techniques, like high-speed videos and photographs (Figure 19) using the lateral or frontal plexiglas windows of the CPRTF (Figure 9).

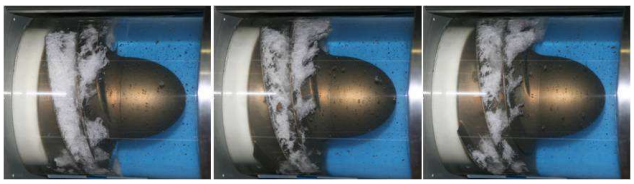

Figure 19 Lateral pictures of DAPAMITO3 inducer in cavitating conditions.

The frontal window has been used for high-speed movies (up to 16000 fps) of the cavitation developed on leading edges of inducer blades. The required illumination level is provided by three halogen lamps with a power of 1250 W located on the sides of the inducer inlet. The high-speed camera can also be synchronized with a stroboscopic light having a maximum flash frequency of 1000 lamps/second. This optical instrumentation can be used for analyzing the cavitating region on the test body and, in particular, for studying in detail the oscillating behavior of the cavity under flow instability conditions, in order to confirm and better understand the results obtained from pressure measurements. To this purpose a dedicated image processing algorithm has been implemented, able to convert all frames of the movies taken under cavitating conditions into simple "black & white" images, where white pixels correspond to the cavitating area and black pixels to the noncavitating region. More in detail, a "threshold" segmentation technique has

been used for separating the cavitating regions from the rest of the image: the pixels having an intensity in the original image greater than a certain threshold value (selected by an appropriate threshold identification method) are set as white, while all other pixels are set as black. The resulting images can therefore be easily analyzed by computational tools, in order to determine the extension and characteristics of the cavitating region as functions of the time. Figure 20 shows an example of a frame before and after the application of the algorithm.

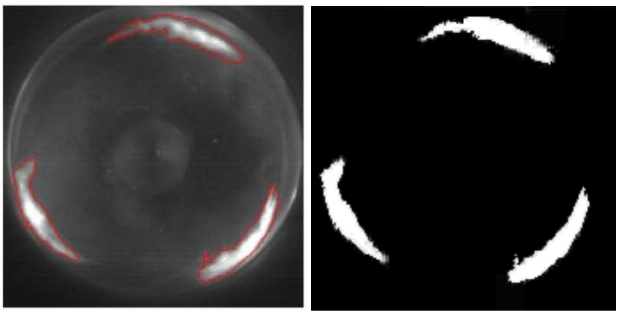

Figure 20 Sample case of comparison between the original frame and the processed binary image obtained by the algorithm developed ([27]).

Rotordynamics

Rotordynamic is one of the most critical aspects of turbomachines, because of possible catastrophic failures due to the development of whirl motions of the pump. In the CPRTF fluid-induced rotordynamic forces are studied using the rotating dynamometer in forced-vibration experiments. A circular whirl orbit with proper eccentricity is imparted to the impeller of the test pump in order to generate and measure the normal ($\vec{F}_N$) and tangential ($\vec{F}_T$) components of the unsteady force acting on the impeller, assess their destabilizing/stabilizing effects on eccentric motion (Figure 21) and determine the rotordynamic matrix of the machine.

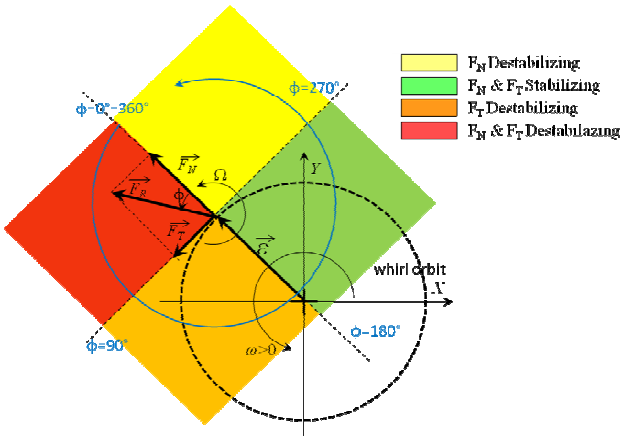

Figure 21 Schematic of the decomposition of the rotordynamic force ($\vec{F}_R$) in its components normal ($\vec{F}_N$) and tangent ($\vec{F}_T$) to the whirl orbit. The colors identify the stabilizing/destabilizing nature of the components of the rotordynamic force in the case of positive whirl ratios.

Two different experimental procedures (discrete and continuous) have been applied for the evaluation of the rotordynamic forces. In discrete tests all of the relevant parameters (ϕ , e and the whirl ratio ω/Ω) are fixed during each experiment. In continuous tests the whirl ratio changes during the experiments in order to slowly span over the range of interest, typically from negative to positive synchronous or supersynchronous values. With this procedure it is possible to obtain all of the relevant experimental information from just one single test. In Figure 22 the (nondimensional) normal and tangential rotordynamic forces obtained with both of the above procedures are compared for the operation of the DAPAMITO4 inducer under non-cavitating conditions. The destabilizing/stabilizing regions for the rotordynamic forces acting on the impeller are shown in orange and green, respectively. The results of the two test procedures are in close agreement, confirming the validity of continuous tests for the more rapid characterization of rotordynamic fluid forces on whirling and cavitating impellers.

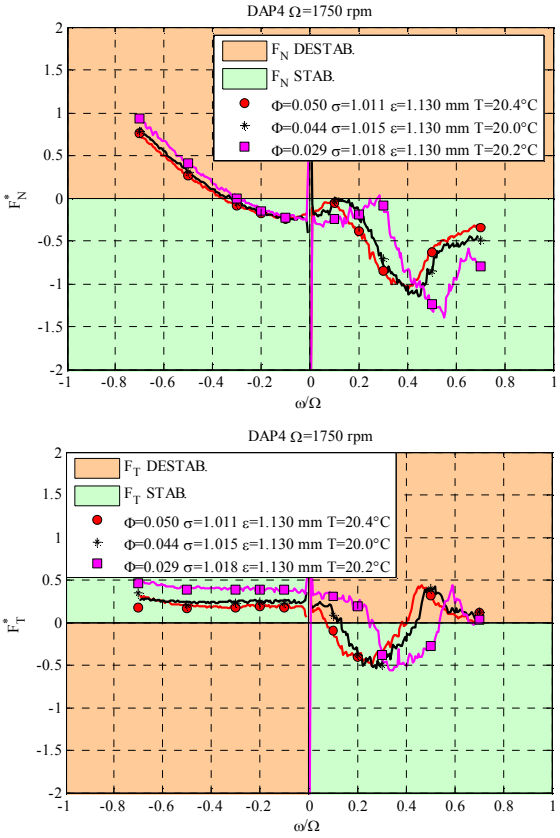

Figure 22 Continuous and discrete tests for the determination of the normal (top) and tangent (bottom) rotordynamic forces acting on DAPAMITO4 inducer at different flow coefficients in non cavitating conditions.

POGO Characterization

Recently the capabilities of Alta's CPRTF have been upgraded in order to conduct experiments for the characterization of the dynamic transfer matrices of turbopumps for space applications. A theoretical analysis has been carried out in order to properly modify the CPRTF configuration ([28]). The setup of the system is quite different from the other configurations used for the same purpose ([26]). Figure 10 shows the rendering of the two test setups (Figure 11 shows the so-called "long" configuration) designed for the experimental campaign, which is currently in progress. For the characterization of the dynamic transfer matrices of turbopumps under cavitating conditions, a vibration table vertically oscillates the water tank. Piezoelectric and differential pressure transducers are used at several stations along the water loop for the measurement of pressure fluctuations, which are used for measuring the pressure and flow rate oscillations at the inlet and discharge cross-section of the turbopump. These quantities, measured in both configurations of the CPRTF under the same operative conditions of the machine, are used for the experimental evaluation of the dynamic transfer matrices. The characterization of the dynamic transfer matrices as a function of the oscillation frequency is obtained by varying the periodicity of the tank vibration used to excite the flow. The experiments can also be carried out at different cavitation levels and at different intensities of thermodynamic effects by varying the pressure and temperature of the flow inside the reservoir in order to highlight the influence of these phenomena on the dynamic response of the turbopump flow to external flow perturbations, as required for the analysis, prediction and control of POGO oscillations in liquid propellant rockets.

CONCLUSIONS

Alta's CPRTF has been presented in this paper. The capabilities of this low cost and easily reconfigurable test facility have been discussed, and in particular: the extension of the range of attainable flow rates in the experimental characterization of cavitating/noncavitating in ducersobtained by means of the introductions of the auxiliary pump, the possibility of conducting focused experiments for the determination of the rotordynamic forces acting on turbopump inducers and impellers by means of an especially designed experimental apparatus, and the ongoing modifications to the CPRTF introduced for enabling the characterization of the dynamic transfer matrices of cavitating turbomachinery . The results clearly demonstrate the rather unique capabilities of Alta's CPRTF for effectively supporting the design of some of the most crucial aspects of today's advanced turbomachinery for space propulsion applications.

ACKNOWLEDGEMENTS

The authors would like to express their gratitude to Profs. Mariano Andrenucci, Renzo Lazzeretti and Fabrizio Paganucci of the Dipartimento di Ingegneria Aerospaziale, Università di Pisa, Italy, for their constant and friendly encouragement. A special acknowledgement goes to Dr. Angelo Cervone, who worked for many years at Alta S.p.A. and significantly contributed to the setup and all of the upgrades of the CPRTF since its original concept and implementation. A special thank goes to the students and colleagues who joined the research group throughout the years, giving their precious

support and invaluable contributions. The present work has been supported by ESA-ESTEC, Noordwijk, The Netherlands, under the Technology Research Program. Finally, the authors would like to express their gratitude to Dr. Giorgio Saccoccia and Dr. Johan Steelant of ESA-ESTEC, who supervised large portions of the activities that led to results presented in this article.

REFERENCES

[1] Stripling L.B. and Acosta A.J., 1962, "*Cavitation in Turbopumps*" – Part 1, ASME J. Basic Eng., Vol. 84, pp. 326-338.

[2] Sack L.E. and Nottage H.B., 1965, "*System Oscillations Associated to Cavitating Inducers*", ASME J. Basic Eng., Vol. 87, pp. 917-924.

[3] Natanzon M.S. el al., 1974, "*Experimental Investigation of Cavitation Induced Oscillations of Helical Inducers*", Fluid Mech. Soviet Res., Vol. 3 No. 1, pp.38-45.

[4] Braisted D.M. and Brennen C.E., 1980, "*Auto-oscillation of Cavitating Inducers*", Polyphase Flow and Transport Technology, ed. R.A. Bajura, ASME Publ., New York, pp. 157-166.

[5] d'Auria F., d'Agostino L. & Brennen C.E., 1994, "*Linearized Dynamics of Bubbly and Cavitating Flows in Cylindrical Ducts*", ASME FED Summer Meeting, Incline Village, NV, USA, June 19-23.

[6] d'Auria F., d'Agostino L. & Brennen C.E., 1995, "*Bubble Dynamic Effects on the Rotordynamic Forces in Cavitating Inducers*", ASME FED Summer Meeting, Hilton Island, SC, USA, August 13-18.

[7] d'Agostino L., & Venturini-Autieri M., 2002, "*Three-Dimensional Analysis of Rotordynamic Fluid Forces on Whirling and Cavitating Finite-Length Inducers*", 9th Int. Symp. on Transport Phenomena and Dynamics of Rotating Machinery (ISROMAC-9), Honolulu, HI, USA, February 10-14.

[8] d'Agostino L. & d'Auria F., 1997, "*Three-Dimensional Analysis of Rotordynamic Forces on Whirling and Cavitating Inducers*", ASME FED Summer Meeting, Vancouver, BC, Canada, June 22-26.

[9] Brennen C.E., 1994, "*Hydrodynamics of Pumps*", Concepts ETI, Inc. and Oxford University Press.

[10] Rosenmann W., 1965, "*Experimental Investigations of Hydrodynamically Induced Shaft Forces with a Three Bladed Inducer*", Proc. ASME Symp. on Cavitation in Fluid Machinery, pp. 172-195.

[11] Jery B. et al., 1985, "*Forces on Centrifugal Pump Impellers*", 2nd Int. Pump Symp., Houston, TX, USA, April 29-May 2, 1985.

[12] Franz R. et al., 1989, "*The Rotordynamic Forces on a Centrifugal Pump Impeller in the Presence of Cavitation*", ASME FED-81, pp. 205-212.

[13] Bhattacharyya A., 1994, "*Internal Flows and Force Matrices in Axial Flow Inducers*", Ph. D. thesis, Div. Eng. & Appl. Science, Caltech, Pasadena, CA, USA.

[14] Rapposelli E., Falorni R. & d'Agostino L., 2002, "*Two-Phase and Inertial Effects on the Rotordynamic Forces in Whirling Journal Bearings*", Proc. 2002 ASME FED Summer Meeting, Montreal, Quebec, Canada, July 14-18.

[15] Rubin S., 1966, "*Longitudinal Instability of Liquid Rockets due to Propulsion Feedback (POGO)*", J. of Spacecraft and Rockets, Vol.3, No. 8, pp.1188-1195.

[16] Rapposelli E., Cervone A. & d'Agostino L.,2002, "*A New Cavitating Pump Rotordynamic Test Facility"*, AIAA Paper 2002-4285, 38th AIAA/ASME/SAE/ASEE Joint Propulsion Conference, Indianapolis, IN, USA, July 8-11.

[17] Ryan R.S., Gross L.A., Mills D., Michell P., 1994, "*The Space Shuttle Main Engine Liquid Oxygen Pump High-Synchronous Vibration Issue, the Problem, the Resolution Approach, the Solution*", AIAA Paper 94-3153, 30th AIAA/ASME/SAE/ASEE Joint Propulsion Conference, Indianapolis, USA.

[18] Goirand B., Mertz A.L., Jousselin F., Rebattet C., 1992, "*Experimental Investigations of Radial Loads Induced by Partial Cavitation with Liquid Hydrogen Inducer*", IMechE, C453/056, pp. 263-269.

[19] Kamijo K., Yoshida M., Tsujimoto Y., 1993, "*Hydraulic and Mechanical Performance of LE-7 LOX Pump Inducer*", AIAA J. Propulsion & Power, Vol. 9, No. 6, pp. 819-826.

[20] Tsujimoto Y., Semenov Y. A., 2002, "*New Types of Cavitation Instabilities in Inducers*", 4th Int. Conf. on Launcher Technology, Liege, Belgium.

[21] Rapposelli E., Cervone A., Bramanti C. & d'Agostino L.,2002, "*A New Cavitation Test Facility at Centrospazio"*, 4th International Conference on Launcher Technology "Space Launcher Liquid Propulsion", Liege, Belgium, December 3-6.

[22] Cervone A., Torre L., Bramanti C., Rapposelli E. & d'Agostino L "*Experimental Characterization of Cavitation Instabilities in the Avio "FAST2" Inducer",* 41th AIAA/ASME/SAE/ASEE Joint Propulsion Conference, Tucson, Arizona, USA, 2005.
[23] Cervone A., Testa R., Bramanti C., Rapposelli E., d'Agostino L., 2005, "*Thermal Effects on Cavitation Instabilities in Helical Inducers*", AIAA Journal of Propulsion and Power, Vol. 21, No. 5, pp. 893-899.
[24] Torre L., Pasini A., Cervone A., and d'Agostino L., 2009, "*Experimental Performance of a Tapered Axial Inducer: Comparison with Analytical Predictions*", 45th AIAA/ASME/SAE/ASEE Joint Propulsion Conf. and Exhibit, Denver, CO, 2-5 August 2009.
[25] Cervone A., Pace G., Torre L., Pasini A., Bartolini S., Agnesi L., d'Agostino L. 2012,"*Effects of the Leading Edge Shape on the Performance of an Axial Three Bladed Inducer*",14th Int. Symp. on Transport Phenomena and Dynamics of Rotating Machinery, ISROMAC-14, February 27th – March 2, 2012, Honolulu, HI, USA.
[26] Ng, S.L. and Brennen, C., 1978, "*Experiments on the dynamic behavior of cavitating pumps*", ASME J. Fluids Eng., 100, No.2, 166-176.
[27] Cervone A., Torre L., Fotino D., Bramanti C. and d'Agostino L., 2006 "*Setup of a high-speed optical system for the characterization of cavitation instabilities in space turbopumps",* 6th International Symposium on Cavitation, Wageningen, The Netherlands.
[28] Cervone A., Torre L., Pasini A., Piccoli E.A., d'Agostino L., 2010,"*Design of a Test Setup for the Characterization of the Dynamic Transfer Matrix of Cavitating Inducers*",46th AIAA/ASME/SAE/ASEE Joint Propulsion Conference & Exhibit, Nashville, TN, USA, July 25 - 28, ISSN: 0146-3705.
[29] d'Agostino L., Torre L., Pasini A., Cervone A., 2008, "*On the Preliminary Design and Noncavitating Performance of Tapered Axial Inducers*", ASME J. of Fluids Engineering, Vol. 130, Is. 11, November 2008, pp. 111303-1/111303-8.
[30] d'Agostino L., Torre L., Pasini A. and Cervone A., 2008, "*A Reduced Order Model for Preliminary Design and Performance Prediction of Tapered Inducers*", 12th Int. Symp. on Transport Phenomena and Dynamics of Rotating Machinery, Honolulu, Hawaii, USA, February 17-22.
[31] d'Agostino L., Torre L., Pasini A., Baccarella D., Cervone A. and Milani A., 2008, "*A Reduced Order Model for Preliminary Design and Performance Prediction of Tapered Inducers: Comparison with Numerical Simulations*", AIAA Paper 5119, 44th AIAA/ASME/SAE/ASEE Joint Propulsion Conf. and Exhibit, Hartford, CT, USA, July 21–23.